

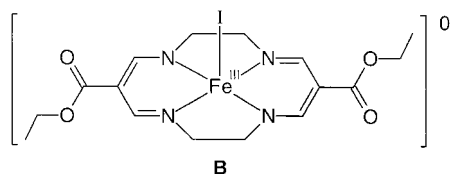
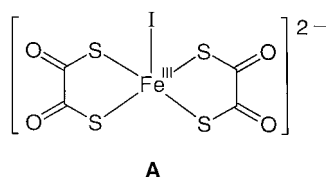
$wR_2 = 0.0822$ (all data). The NH proton was refined freely, methyl H atoms as rigid, and other H atoms as a riding model. Crystallographic data (excluding structure factors) for the structure reported in this paper have been deposited with the Cambridge Crystallographic Data Centre as supplementary publication no. CCDC-154120. Copies of the data can be obtained free of charge on application to CCDC, 12 Union Road, Cambridge CB2 1EZ, UK (fax: (+44) 1223-336-033; e-mail: deposit@ccdc.cam.ac.uk).

[11] G. Muges, A. Panda, H. B. Singh, N. S. Puneekar, R. J. Butcher, *J. Am. Chem. Soc.* **2001**, *123*, 839.

Tuning the Electronic Structure of Halidobis(*o*-imino-benzosemiquinonato)-iron(III) Complexes**

Hyunghil Chun, Thomas Weyhermüller, Eckhard Bill, and Karl Wieghardt*

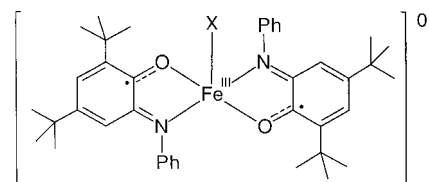
Mononuclear complexes of iron(III) (d^5) containing redox-inert, closed-shell ("innocent") ligands adopt either a high-, intermediate-, or low-spin electron configuration: $S_{Fe} = 5/2$, $3/2$, or $1/2$, respectively. An increasing number of non-heme, pentacoordinate, pure intermediate-spin complexes have in recent years been characterized by X-ray crystallography, magnetic susceptibility measurements, Mössbauer, and electron paramagnetic resonance (EPR) spectroscopy.^[1] Examples pertinent to this work are complexes **A**^[1f] and **B**.^[1d]



The binding of a Fe^{III} ion to open-shell ("noninnocent"), π -radical ligands such as phenoxyls^[2a] or *o*-benzosemiquinonates^[2b] inevitably induces a strong intramolecular, antiferromagnetic spin coupling between the magnetic orbitals of the π radicals and the available metal-centered, half-filled t_{2g} orbitals of the Fe^{III} ion. This gives rise to electronic ground states ranging from $S_t = 2$ ^[2a,b] to $S_t = 0$ ^[2c] depending on the number of coordinated radicals and the actual local spin state at the Fe^{III} ion in a given compound. *O,N*-coordinated *o*-

aminophenolates have been shown to be readily oxidized by air to yield the corresponding *o*-iminobenzosemiquinonates, $(L^{ISO})^-$.^[3, 4] The octahedral complex $[Fe^{III}(L^{ISO})_3]$ possesses an $S_t = 1$ ground state comprising a high-spin Fe^{III} ion ($S_{Fe} = 5/2$) coupled antiferromagnetically to three $(L^{ISO})^-$ π -radical ligands.^[3b]

We have now discovered that the pentacoordinate halidobis(*o*-iminosemiquinonato)iron(III) complexes **1–3** are readily prepared and that the local spin state of the respective Fe^{III}



X = Cl, Br, I

trans- $[Fe(L^{ISO})_2Cl]$ **1**

trans- $[Fe(L^{ISO})_2Br]$ **2**

trans- $[Fe(L^{ISO})_2I]$ **3**

ion is tuned from a high-spin state in the chloro species **1** to a pure intermediate-spin state in the iodo complex **3**; in the bromo analogue **2** both spin isomers are present in the crystalline state in a 1:1 ratio. The crystal structures of **1**, **2**, and **3** have been determined with high precision by X-ray crystallography at 100 K. Figure 1 shows the structure of **3** (the structures of **1** and **2** are very similar and not shown); Table 1 summarizes selected bond lengths.

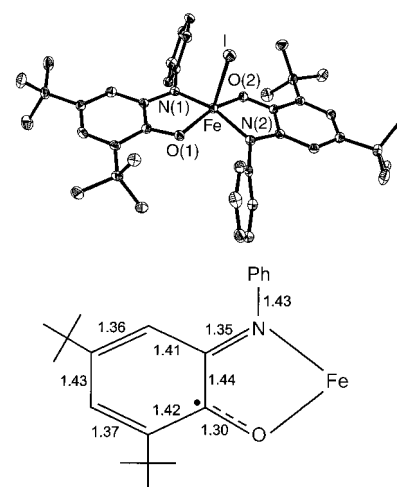


Figure 1. Structure of a neutral molecule in crystals of **3** ($S_t = 1/2$; top). The average C–C, C–O, and C–N bond lengths of the *o*-iminobenzosemiquinonato(1 –) π -radical ligand in **1**, **2**, and **3** are shown below. The estimated error is ± 0.01 Å (3σ).

Table 1. Selected bond lengths [Å] in **1**, **2**, **3**, and $[Fe("N_2S_2")I]$.^[c]

	Fe–X	Fe–N(1)	Fe–N(2)	Fe–O(1)	Fe–O(2)
$[Fe^{III}(L^{ISO})_2Cl]$ 1	2.2203(7)	2.042(2)	2.041(2)	1.962(1)	1.964(1)
$[Fe^{III}(L^{ISO})_2Br]$ 2 ^[a]	2.3665(9)	1.897(4)	1.886(4)	1.869(3)	1.877(3)
$[Fe^{III}(L^{ISO})_2Br]$ 2 ^[b]	2.3694(9)	2.045(4)	2.050(4)	1.950(3)	1.953(3)
$[Fe^{III}(L^{ISO})_2I]$ 3	2.5912(5)	1.885(2)	1.885(2)	1.869(1)	1.881(1)
$[Fe("N_2S_2")I]$ ^[c]	2.5552(9)	1.842(4)	1.851(5)	2.181(2)	2.188(2)

[a] Molecule 1. [b] Molecule 2. [c] Fe–S bond length.

[*] Prof. Dr. K. Wieghardt, Dr. H. Chun, Dr. T. Weyhermüller, Dr. E. Bill
Max-Planck-Institut für Strahlenchemie
Stiftstrasse 34–36, 45470 Mülheim an der Ruhr (Germany)
Fax: (+49) 208-306-3952
E-mail: wieghardt@mpi-muelheim.mpg.de

[**] This work was supported by the Fonds der Chemischen Industrie. H. Chun thanks the Alexander von Humboldt Foundation for a stipend.

It is important to note that the geometrical details of the *O,N*-coordinated (L^{ISO})[−] ligand are identical in all three structures within our small 3σ limits of ± 0.01 Å; the average C–O, C–N, and C–C bond lengths are given in Figure 1. These values are consistent with those of all other complexes of this type reported to date.^[3, 4] Thus, in complexes **1–3** the ligand is always an *o*-iminosemiquinonate(1[−]) radical with $S_{rad} = \frac{1}{2}$.^[3, 4]

A comparison of the Fe–O and Fe–N distances in **1** and **3** (Table 1) reveals that the Fe^{III} ions in the neutral $[Fe^{III}(L^{ISO})_2X]$ ($X = Cl, I$) molecules must possess different local spin states, since these distances are long in **1**, but significantly shorter in **3**. Compound **2** crystallizes in the triclinic space group $P\bar{1}$ with $Z = 4$, indicating that two crystallographically independent molecules of $[Fe^{III}(L^{ISO})_2Br]$ are present in the unit cell. The Fe–N and Fe–O bond lengths of the first molecule match those in **3** and those of the second molecule are identical to those in **1**. Thus, crystals of **2** contain a 1:1 mixture of two spin isomers of $[Fe^{III}(L^{ISO})_2Br]$. As we will show below, **1** contains a high-spin and **3** a pure intermediate-spin iron center, whereas solid **2** contains both isomers in a ratio 1:1.

Variable-temperature magnetic susceptibility measurements on solid samples of **1**, **2**, and **3** have been performed by using a SQUID magnetometer (external field 1 T). Figure 2 shows the temperature dependence of the effective

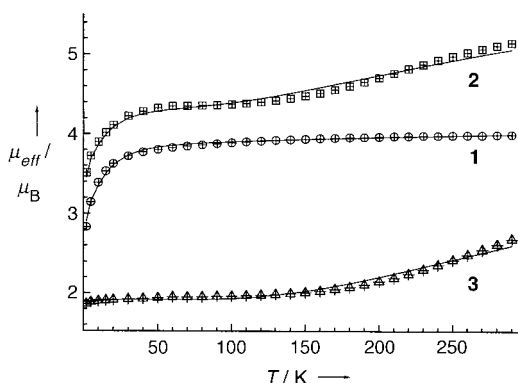


Figure 2. Temperature dependence of the effective magnetic moment μ_{eff} as calculated per *one* Fe ion for **1** and **3**, and per *two* Fe ions (double molecular weight) for **2**.

magnetic moments, where we have calculated μ_{eff} per *one* Fe ion for **1** and **3**, but per *two* Fe ions for **2**. The curve obtained for **1** is readily simulated for an $S_t = \frac{3}{2}$ ground state with a zero-field splitting parameter $|D_{3/2}|$ of 18 cm^{-1} and an effective g value of 2.0 (fixed). The X-band EPR spectrum of a frozen CH_2Cl_2 solution of **1** at 10 K (Figure 3) displays a typical $S_t = \frac{3}{2}$ signal with small rhombicity ($E/D \approx 0$).

In contrast, solid **3** displays a temperature-independent μ_{eff} of about $1.9\mu_B$ in the range 10–150 K; above 150 K μ_{eff} increases to $2.7\mu_B$ per Fe^{III} ion at 300 K. Complex **3** clearly possesses an $S_t = \frac{1}{2}$ ground state. The temperature dependence (see Figure 2) was successfully modeled by assuming intramolecular coupling of the two radical ligands $S_{rad} = \frac{1}{2}$ with a central intermediate-spin Fe^{III} ion, $S_{Fe} = \frac{3}{2}$, by using the spin Hamiltonian $\mathcal{H} = -2JS_{rad}S_{Fe}$. A strong antiferromag-

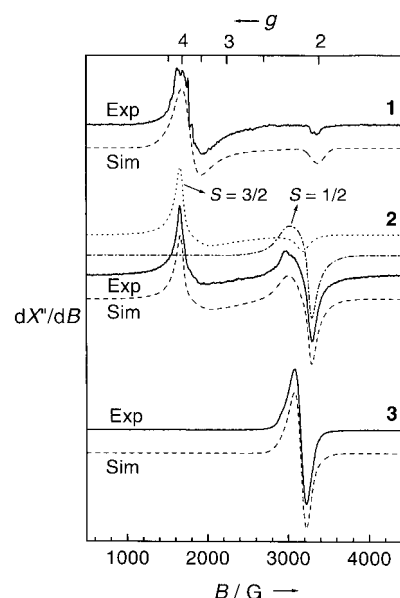


Figure 3. X-band EPR spectra of frozen CH_2Cl_2 solutions of **1**, **2**, and **3**. The dotted lines represent simulations (Sim, Table 2). Conditions: $T = 10\text{ K}$, frequency = 9.47 GHz ; power = $100\text{ }\mu\text{W}$ for **1** and **2**, $50\text{ }\mu\text{W}$ for **3**; modulation amplitude = 10 G for **1** and **2**, 31 G (for **3**).

netic coupling of $J = -145(20)\text{ cm}^{-1}$ is typical for such complexes.^[2] In agreement with these results, the EPR spectrum of **3** in frozen CH_2Cl_2 solution at 10 K displays an axial $S_t = \frac{1}{2}$ signal which was satisfactorily simulated with $g_{\parallel} = 2.189$ and $g_{\perp} = 2.134$ (Figure 3). These g values indicate that the unpaired electron in **3** resides in a metal-centered *d* orbital.

Compound **2** displays a fascinating temperature dependence of μ_{eff} which is nearly temperature independent at $4.3\mu_B$ in the range 50–150 K; below 50 K it decreases to $3.5\mu_B$ at 4 K due to zero-field splitting of the $S_t = \frac{3}{2}$ component, but increases above 150 K to $5.2\mu_B$ at 300 K due to decoupling of the spins of the $S_t = \frac{1}{2}$ component. The $4.3\mu_B$ value corresponds nicely to the expected value of $4.2\mu_B$ calculated for a 1:1 mixture of an $S_t = \frac{1}{2}$ and an $S_t = \frac{3}{2}$ system by using the simple relation $\mu_{eff} = (\mu_1^2 + \mu_2^2)^{1/2}$ with $\mu_1 = 1.73\mu_B$ and $\mu_2 = 3.87\mu_B$. For the $S_t = \frac{1}{2}$ component a coupling constant J of $-100(20)\text{ cm}^{-1}$; and for the $S_t = \frac{3}{2}$ state a zero-field splitting parameter of $|D_{3/2}| = 18\text{ cm}^{-1}$ was established from the fit shown in Figure 2. The EPR spectrum of **2** in frozen CH_2Cl_2 at 10 K (Figure 3) shows signals due to an $S_t = \frac{3}{2}$ and an $S_t = \frac{1}{2}$ system. The ratio of the two species *in solution* was found to be about 7:3 in the temperature range 2–35 K. The relative abundance of both spin isomers in **2** might be an arbitrary “frozen” Boltzmann distribution prevailing in fluid solution, whereas in the solid state this distribution is fixed at 1:1.

The zero-field Mössbauer spectra of solid samples of **1**, **2**, and **3** provide independent spectroscopic information on the local spin and oxidation states of the iron ions (Table 2); the spectra recorded at 80 K are shown in Figure 4. Complexes **1** and **3**^[5] exhibit each a *single* quadrupole doublet where the large isomer shift for **1** indicates the presence of a high-spin Fe^{III} ion ($S_{Fe} = \frac{5}{2}$), and, for **3**, the smaller value is typical for a

Table 2. X-band EPR and Mössbauer parameters.

Complex	$S_1^{[a]}$	g_1	g_2	g_3	δ [mm s ⁻¹] ^[b]	$ \Delta E_Q $ [mm s ⁻¹] ^[c]	T [K] ^[d]
1	$\frac{3}{2}$	3.985	3.871	2.010	0.45	1.26	80
2	$\frac{3}{2}$	4.030	3.643	2.130	0.47	1.22	80
	$\frac{1}{2}$	2.272	2.105	2.071	0.23	2.62	80
3	$\frac{1}{2}$	2.189(g_{\parallel}), 2.134(g_{\perp})			0.24	2.80	80
A ^[1f]	$\frac{3}{2}$		ca. 4		0.30	3.5	77
B ^[1d]	$\frac{3}{2}$	5.38	2.70	1.74	0.18	3.56	120
[Fe("N ₂ S ₂ ")I] ^[6]	$\frac{1}{2}$	2.206	2.125	2.063	0.11	3.41	4.2
[Fe(L ^{ISO}) ₃] ^[3b]	1				0.54	1.03	80

[a] Ground state. [b] Isomer shifts versus α -Fe at 298 K. [c] Quadrupole splitting. [d] Measurement temperature for the Mössbauer spectra.

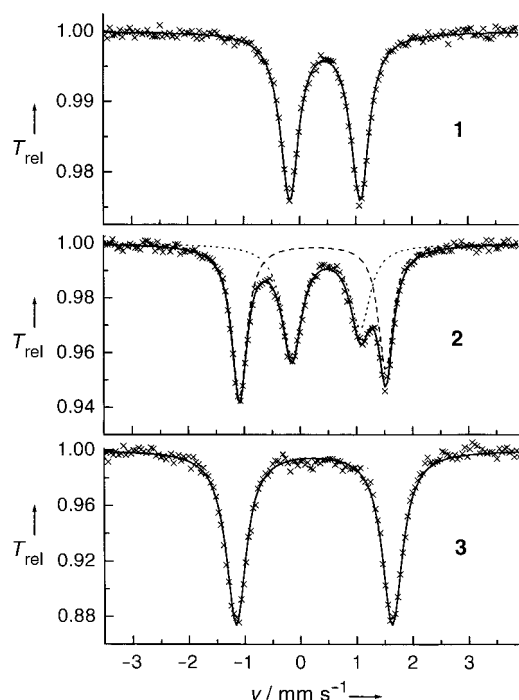


Figure 4. Zero-field Mössbauer spectra of solid samples of **1**, **2**, and **3** measured at 80 K (parameters see Table 2).

pure intermediate-spin Fe^{III} species ($S_{Fe} = \frac{3}{2}$).^[1] We note that the large quadrupole splitting of **1** as well as the large zero-field splitting are typical of high-spin, five-coordinate Fe^{III} complexes with some spin admixture ($S = \frac{5}{2} \leftrightarrow S = \frac{3}{2}$) due to the presence of a close lying excited spin quartet state which is mixed into the $S = \frac{5}{2}$ ground state. This situation is also clearly reflected in the low average value $(g_1 + g_2)/2 = 3.93$ which would be 4.0, if the spin of the central Fe^{III} ion in **1** would be purely $S = \frac{5}{2}$.

Consistent with the X-ray structure analysis, the spectrum of **2** displays two distinctly different quadrupole doublets (ratio 53:47 ~ 1:1; Figure 4); the isomer shifts correspond to those of a high-spin (as in **1**) and an intermediate-spin Fe^{III} ion (as in **3**).

We have shown that in a series of isostructural complexes the local spin-state of the central Fe^{III} ion is $\frac{5}{2}$ in **1**, $\frac{5}{2}$ and $\frac{3}{2}$ in **2**, and purely $\frac{3}{2}$ in **3**. This fine-tuning is governed by the nature of the halide ion in apical position.^[1a] Coupling of these Fe^{III} ions to two π -radical ligands yields the observed ground states: $S_1 = \frac{3}{2}$ for **1**, $\frac{3}{2}$ and $\frac{1}{2}$ for **2**, and $\frac{1}{2}$ for **3**.

In the light of the above results we would like to offer an alternative description of the electronic structure of the structurally very similar complex [Fe("N₂S₂")I] reported by Sellmann et al.^[6] which is shown in Figure 5. These authors

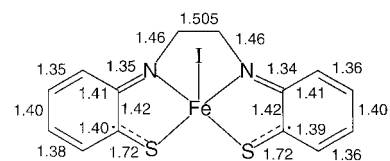


Figure 5. Schematic representation of the structure of [Fe("N₂S₂")I].^[6] The bond lengths were obtained from the Cambridge Crystallographic Data Centre: no. CCDC-100299. The estimated error of the C–C, C–S, and C–N bond lengths is ± 0.02 Å (3σ).

considered the ligand 1,2-ethanediamide-*N,N'*-bis(2-benzenethiolate)(4-), "N₂S₂", to be a redox-innocent, closed-shell tetraanion and, consequently, have assigned a formal oxidation state of +v to the iron center. This species possesses an $S_1 = \frac{1}{2}$ ground state like **3**. In our view the spectroscopic (or physical) oxidation state^[7] of the central iron ion in this complex is +III. An intermediate-spin Fe^{III} ion ($S_{Fe} = \frac{3}{2}$) is *N,S*-coordinated to two *o*-iminothionebenzo-semiquinonato(1-) π radicals ($S_{rad} = \frac{1}{2}$) which couple anti-ferromagnetically to the t_{2g}^4 subshell of the Fe^{III} ion ($d_{xy}^2, d_{xz}^1, d_{yz}^1, d_{z^2}^1$) yielding the observed metal-centered $S_1 = \frac{1}{2}$ ground state ($d_{z^2}^1$) as in **3**. This proposal is supported by the following experimental data:^[6] 1) The two *N,S*-coordinated ligand parts of "N₂S₂" display the same geometrical distortions which are reported here for the (L^{ISO})⁻ ligands in **3**: the C–S bonds are short (1.72 Å) and approach the length for a C=S double bond, as are the C–N bonds (1.35 Å). In addition, although not quite beyond their experimental 3σ error limits, both phenyl rings display typical quinoid-type distortions. 2) The Mössbauer parameters (see Table 2) are in excellent agreement with those reported for complexes **2**, **3**, **A**, and **B** all of which contain an intermediate-spin Fe^{III} ion. 3) The EPR spectra for [Fe("N₂S₂")I] and **3** are very similar.

Experimental Section

The ligand 2-anilino-4,6-di-*tert*-butylphenol, H[L^{AP}], has been prepared as described previously.^[3]

Syntheses of complexes: The ligand H[L^{AP}] (1.5 mmol) and triethylamine (3 mmol) dissolved in methanol (20 mL) or ethanol/dichloromethane (1/1) were added the ferrous salts (1 mmol) FeCl₂·4H₂O, FeBr₂, or FeI₂ in methanol (30 mL). Triphenylphosphane (2 mmol) was additionally added to the reaction mixtures of **2** and **3** to facilitate crystallization. The solution was heated to reflux in the presence of air for 1 h. After filtration, the solution was allowed to stand at ambient temperature for two to three days whereupon dark crystalline precipitates formed which were collected by filtration and washed with cold methanol and acetone. Yields: **1**: 0.51 g (88 %); **2**: 0.21 g (38 %); **3**: 0.39 g (67 %). Elemental analyses (%) calcd for C₄₀H₅₀N₂O₂ClFe: C 70.43, H 7.39, N 4.11, Cl 5.20; found: C 70.26, H 7.37, N 4.13, Cl 5.23; calcd for C₄₀H₅₀N₂O₂BrFe: C 66.12, H 6.94, N 3.86, Br 11.00; found: C 65.94, H 7.08, N 3.78, Br 10.90; calcd for C₄₀H₅₀N₂O₂IFe: C 62.10, H 6.51, N 3.62, I 16.40; found: C 61.86, H 6.42, N 3.57, I 16.26. EI mass spectra showed the correct molecular ion peak at m/z 681 for [**1**]⁺, 727 for [**2**]⁺, and 773 for [**3**]⁺. EPR, Mössbauer, and magnetic susceptibility equipment and procedures for simulation of data are the same as described in ref. [2a].

Crystal structure analysis data for **1**: $C_{40}H_{50}N_2O_2ClFe$, $M_r = 682.12$, triclinic, $P\bar{1}$, $a = 10.738(1)$, $b = 13.195(1)$, $c = 14.061(1)$ Å, $\alpha = 75.19(1)$, $\beta = 79.71(1)$, $\gamma = 77.80(1)^\circ$, $V = 1866.1(3)$ Å³, $Z = 2$, $\rho_{\text{calcd}} = 1.214$ Mg m⁻³; $\mu(\text{Mo}_{K\alpha}) = 0.511$ mm⁻¹, $F(000) = 726$; 18080 reflections collected at 100(2) K; 9891 independent reflections; $GOF = 0.990$; $R = 0.0508$; $wR2 = 0.1059$. Crystal structure analysis data for **2**: $C_{40}H_{50}N_2O_2BrFe$, $M_r = 726.58$, triclinic, $P\bar{1}$, $a = 10.4544(9)$, $b = 14.737(1)$, $c = 24.387(2)$ Å, $\alpha = 86.88(2)$, $\beta = 84.89(2)$, $\gamma = 87.58(2)^\circ$, $V = 3734.0(5)$ Å³, $Z = 4$, $\rho_{\text{calcd}} = 1.292$ Mg m⁻³; $\mu(\text{Mo}_{K\alpha}) = 1.509$ mm⁻¹, $F(000) = 1524$; 29363 reflections collected at 100(2) K; 12766 independent reflections; $GOF = 0.949$; $R = 0.0552$; $wR2 = 0.1030$. Crystal structure analysis data for **3**: $C_{40}H_{50}N_2O_2IFe$, $M_r = 773.57$, monoclinic, $P2_1/c$, $a = 13.497(1)$, $b = 26.326(2)$, $c = 11.672(1)$ Å, $\beta = 112.99(2)^\circ$, $V = 3817.9(6)$ Å³, $Z = 4$, $\rho_{\text{calcd}} = 1.346$ Mg m⁻³; $\mu(\text{Mo}_{K\alpha}) = 1.238$ mm⁻¹, $F(000) = 1596$; 38047 reflections collected at 100(2) K; 12090 independent reflections; $GOF = 1.007$; $R = 0.039$; $wR2 = 0.072$. Crystallographic data (excluding structure factors) for the structures reported in this paper have been deposited with the Cambridge Crystallographic Data Centre as supplementary publication no. CCDC-159894 (**1**), CCDC-159895 (**2**), and CCDC-159896 (**3**). Copies of the data can be obtained free of charge on application to CCDC, 12 Union Road, Cambridge CB21 1EZ, UK (fax: (+44) 1223-336-033; e-mail: deposit@ccdc.cam.ac.uk).

Received: March 13, 2001 [Z16765]

- [1] a) S. Koch, R. H. Holm, R. B. Frankel, *J. Am. Chem. Soc.* **1975**, 97, 6714; b) D. P. Riley, D. H. Busch, *Inorg. Chem.* **1984**, 23, 3235; c) K. L. Kostka, B. G. Fox, M. P. Hendrich, T. J. Collins, C. E. F. Rickard, L. J. Wright, E. Münck, *J. Am. Chem. Soc.* **1993**, 115, 6746; d) H. Keutel, I. Käßpinger, E.-G. Jäger, M. Grodzicki, V. Schünemann, A. X. Trautwein, *Inorg. Chem.* **1999**, 38, 2320; e) E.-G. Jäger, H. Keutel, *Inorg. Chem.* **1997**, 36, 3512; f) D. Nicarchos, A. Kostikas, A. Simopoulos, D. Coucouvanis, D. Piltingsrud, R. E. Coffman, *J. Chem. Phys.* **1978**, 69, 4411.
- [2] a) M. D. Snodin, L. Ould-Moussa, U. Wallmann, S. Lecomte, V. Bachler, E. Bill, H. Hummel, T. Weyhermüller, P. Hildebrandt, K. Wieghardt, *Chem. Eur. J.* **1999**, 5, 2554; b) R. M. Buchanan, S. L. Kessel, H. H. Downs, C. G. Pierpont, D. N. Hendrickson, *J. Am. Chem. Soc.* **1978**, 100, 7894; c) W. O. Koch, V. Schünemann, M. Gerdan, A. X. Trautwein, H.-J. Krüger, *Chem. Eur. J.* **1998**, 4, 1255.
- [3] a) P. Chaudhuri, C. N. Verani, E. Bill, E. Bothe, T. Weyhermüller, K. Wieghardt, *J. Am. Chem. Soc.* **2001**, 123, 2213; b) H. Chun, C. N. Verani, P. Chaudhuri, E. Bothe, E. Bill, T. Weyhermüller, K. Wieghardt, *Inorg. Chem.*, in press.
- [4] C. N. Verani, S. Gallert, E. Bill, T. Weyhermüller, K. Wieghardt, P. Chaudhuri, *Chem. Commun.* **1999**, 1747.
- [5] We have also recorded the Mössbauer spectrum of **3** at 298 K; a single quadrupole doublet is observed ($\delta = 0.22$ mm s⁻¹, $|\Delta E_Q| = 2.21$ mm s⁻¹). This clearly establishes that the increasing magnetic moment at temperatures > 100 K for **3** (Figure 2) is not due to a spin crossover $S_t = 1/2 \rightarrow S_t = 3/2$.
- [6] D. Sellmann, S. Emig, F. W. Heinemann, *Angew. Chem.* **1997**, 109, 1808; *Angew. Chem. Int. Ed. Engl.* **1997**, 36, 1734.
- [7] C. K. Jørgensen, *Struct. Bonding (Berlin)* **1966**, 1, 234.

Separation of Enantiomers by Extraction Based on Lipase-Catalyzed Enantiomer-Selective Fluorous-Phase Labeling**

Benno Hungerhoff, Helmut Sonnenschein, and Fritz Theil*

Lipase-mediated kinetic resolution of racemic alcohols and their esters by esterification or hydrolysis, respectively, is a well-established method for the preparation of enantiomerically pure or enriched building blocks.^[1] Lipases are cheap biocatalysts; the reactions can be run with standard equipment and are highly selective in many cases. However, there is one major drawback of this type of biotransformation, which affords one of the enantiomers as an alcohol and the other one as the corresponding carboxylate: The products must be separated by chromatography. This separation step may not be a serious problem on the laboratory scale. However, on a large scale in the pharmaceutical industry, a chromatographic step might be the reason this method is not considered to be a useful access to enantiomerically pure intermediates. Until now, there has been no general solution to overcome this disadvantage.

On the other hand, remarkable progress has been made for the extractive separation of homogeneous catalysts,^[2] reagents, and products^[3] equipped with perfluorinated auxiliary groups. This methodology is based on partitioning between the organic and fluorous phases in order to improve the recovery of the homogeneous catalyst and the isolation of products from the reaction mixture.

From the progress made in performing reactions in fluorous media and/or improving workup procedures by the introduction of a fluorous phase,^[4] the following question arises: Is it possible to apply a highly fluorinated acyl donor to a lipase-catalyzed kinetic resolution of a racemic alcohol? Such an acyl donor should promote lipase-mediated enantiomer-selective acyl transfer onto the faster-reacting enantiomer and, thereby, simultaneously label it. This labeled enantiomer with a "teflon ponytail"^[2b] could then be recognized selectively by a fluorous phase, to allow the extractive separation of the fluorinated and nonfluorinated enantiomers between a fluorous and an organic solvent.

For a successful realization of this principle a suitable acyl donor is required. This reagent should be accepted by the lipase forming the reactive acyl enzyme, that subsequently reacts in an enantiomer-selective manner with a racemic alcohol. Furthermore, the transferred acyl residue should have a sufficient fluorine content to allow selective separation of the fluorinated ester from the nonfluori-

[*] Dr. F. Theil, Dr. B. Hungerhoff
ASCA GmbH
Richard-Willstätter-Strasse 12, 12489 Berlin (Germany)
Fax: (+49) 30-6392-4103
E-mail: theil@asca-berlin.de
Dr. H. Sonnenschein
Institut für Nichtklassische Chemie an der Universität Leipzig
Permoserstrasse 15, 04303 Leipzig (Germany)

[**] This work was supported by the Deutsche Forschungsgemeinschaft (grant: TH 562/3-1) and the Fonds der Chemischen Industrie.